EFFECTS OF THE OXIDE LAYER ON PRESSURE INFILTRATION OF PACKED CERAMIC PARTICULATE BY ALUMINUM ALLOYS

C. García-Cordovilla[1], J. Narciso[2], R. Arpón[2], V. Ferrández[2] and E. Louis[3]

[1] *Industria Española del Aluminio, Centro de Investigación y Desarrollo, Apartado 25, E-03080 Alicante, Spain.*
[2] *Departamento de Química Inorgánica, Universidad de Alicante, Apartado 99, E-03080 Alicante, Spain.*
[3] *Departamento de Física Aplicada, Universidad de Alicante, Apartado 99, E-03080 Alicante, Spain.*

SUMMARY: Previous experimental results for the threshold pressure P_0 for infiltration of packed Al_2O_3 particulate by Al-Sn and Al-Pb alloys indicate that both lead and tin decrease P_0 in an amount roughly proportional to the decrease in the liquid vapor surface tension γ_{lv} of liquid aluminum promoted by those elements. Instead, phenomenological theories and contact angle θ data, obtained at low oxygen partial pressure, indicate that the product $\gamma_{lv} \cos \theta$ remains almost constant upon lead or tin additions. As P_0 is proportional to the latter product, we conclude that theories that do not consider the role of the oxide layer or data obtained under low oxidation conditions are useless to analyze pressure infiltration experiments. Experimental results for Al-Mg and Al-Sr alloys further suggest that the oxide layer plays a crucial role in the infiltration process.

KEYWORDS: Metal Matrix Composites, Infiltration, Aluminum Alloys, Ceramic particulate

INTRODUCTION

There is a long standing discussion concerning the effects of the oxide layer on pressure infiltration of ceramic preforms (fibre or particulate) by liquid aluminum [1-5]. A variety of experimental studies indicate that wetting at the aluminium/ceramic interface can be significantly improved by means of procedures addressed to disrupt or weaken the oxide layer that commonly covers liquid aluminium. For instance it has been reported that, reducing the oxygen partial pressure [4], increasing the infiltration temperature [3], or adding chemicals that partially dissolve the oxide layer [2], decrease the threshold pressure for infiltration. In this work we reinterpret previous experimental results for Al-Sn and Al-Pb alloys [6] and analyze new data for Al-Mg and Al-Sr alloys with the aim of clarifying this question.

MATERIALS AND EXPERIMENTAL PROCEDURES

Materials

The alloys investigated in this work were prepared in alumina crucibles of 45 mm internal diameter x 72 mm height. Aluminum of approximately 99.98wt% purity was used all throughout; typical amounts of impurities (wt%) are 0.015 Si and 0.005 Fe. Al-Mg and Al-Sr alloys were prepared from magnesium and strontium master alloys. The characteristics of the Al_2O_3 and SiC particulate used in this work are summarized in Table 1. The average diameters *D* of the particulate were determined by laser light scattering using a Malvern Mastersizer. The indices of refraction of silicon carbide and alumina particulate used in these determinations were 2.67 and 1.7, respectively. The average diameter and the span of the size distribution are given in Table 1. SiC particulate had a non-spherical, angular, shape, whereas alumina particulate were in the form of platelets.

Table 1: Characteristics of the SiC (99.5%) and Al_2O_3 (99.0%) particulate used in this work. *D* is the average diameter (in μm) and V_p the particle volume fraction. The span of the size distribution given by *[D(90)-D(10)]/D*, where *D(10)* and *D(90)* are the diameters below which 10% and 90% of the particles are found, is also reported

Particulate	Type/Shape	Purity	*D*	Span	V_p
SiC	Green	99.5%	26	0.8	0.57
Al_2O_3	Platelets	99.0%	18	1.1	0.58

Experimental Apparatus and Procedures

The infiltration experiments were carried out in a pressure chamber that was described in detail in Ref. [4]. Here we shall only outline its main features. It was made of stainless steel, and can support a maximum pressure of 3000 kPa. A resistance furnace was located inside the chamber. Pressure was measured with a transmitter, and controlled within ±2 kPa. All pressures are referred to atmospheric pressure.

The particulate were packed into quartz tubes of 5 mm I.D. x 20 cm length. At each packing step, approximately 0.04 g of particulate were added, there were applied 3 seconds of vibrations to break layering, and the powder was subjected to 20 strokes of a 35 g weigth from a constant height (10 cm). The procedure was repeated until the compact reached a height of ≈ 3.5 cm. In order to determine the particle volume fraction V_p, the quartz tube was weighed before and after the powder was packed inside it, and its diameter measured at five points along its perimeter. Then a measure of the length of the packed powder allowed to obtain V_p. The densities of the alumina and silicon carbide particulate used in these determinations were 3.9 and 3.21 $g.cm^{-3}$, respectively. The melt side of the compact was plugged with alumina paper 6% of theoretical density, to avoid depacking and skim off the alumina scum during infiltration. A ceramic rod was placed on the top of the preforms to prevent them from moving upwards in the quartz tube during infiltration.

The infiltrations were carried out at a melt temperature of 750º±2ºC. The metal surface was

cleaned just before the immersion of the quartz tube containing the packed specimens. No inert gas was introduced into the packed powder [5]. The chamber was closed and the tube held in the melt for 3 minutes. Pressure was then applied with nitrogen gas at a rate of 50-60 $kPa.s^{-1}$, up to the chosen pressure. After a fixed period of time (120 s in the present work), the chamber was vented at a rate of 30-70 $kPa.s^{-1}$. The sample was taken out of the melt and air cooled, it was sectioned and the infiltration height measured with a precision gauge.

EXPERIMENTAL RESULTS

Summary of previous results for Al-Sn and Al-Pb alloys

The results for the threshold pressure for infiltration of packed SiC and Al_2O_3 particulate with Al-Sn and Al-Pb alloys [6] are illustrated in Table 2. The surface tension of the alloys [7,8] is also shown in the Table. The experimental results indicate that both lead and tin additions decrease the threshold pressure for infiltration in an amount which is almost proportional to the change in the surface tension promoted by these two elements [6]. Effects due to possible changes in wetting seem to be much weaker.

Table 2: Threshold pressures P_0 (in kPa) for infiltration into packed alumina and SiC particulate at T= 750ºC, for the Al alloys investigated in this work. γ_{lv} is the surface tension of the liquid metal ($mN.m^{-1}$) reported in Refs. [7-9]. Threshold pressure data for Al-Sn and Al-Pb are taken from Ref. [6].

Alloy	γ_{lv} (mJ m-2)	P_0 (Al_2O_3)	P_0 (SiC)
Al	862	853	560
Al – 5wt% Sn	731	720	439
Al – 0.5wt% Pb	708	766	422
Al – 0.7wt% Sr	719	-	630
Al – 4 wt% Mg	805	925	520

Al-Sr/SiC system

The experimental results for the infiltrated height versus applied pressure for the Al-Sr alloy are shown in Fig. 1, whereas the estimated value of P_0 is given in Table 2. The results clearly indicate that Sr additions increase the threshold pressure. Preliminar data for an alloy with 2.0 wt% of Sr confirm this trend. As opposed to the case of Al-Sn and Al-Pb, the decrease in P_0 occurs despite of the fact that Sr sharply decrease the surface tension of pure aluminium (see Table 2).

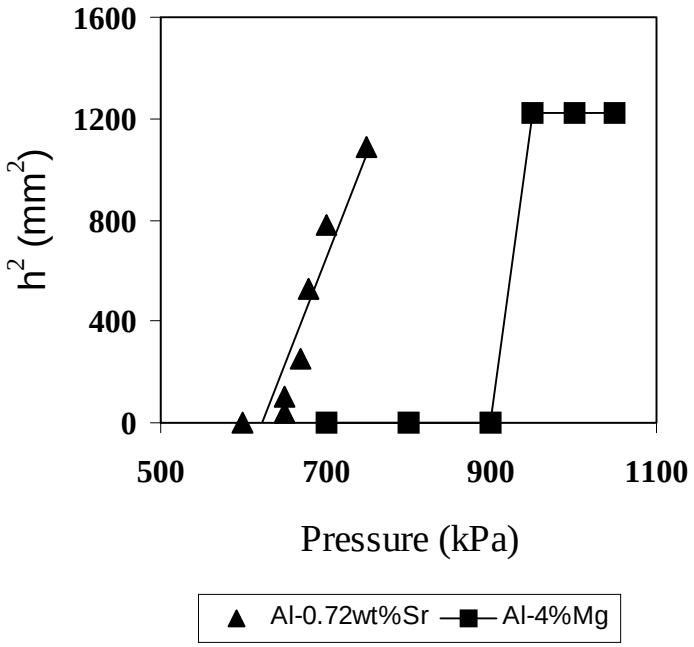

Fig. 1: Square of the infiltrated height as a function of the applied pressure (infiltration time 120 s and infiltration Temperature 750ºC) for packed samples of SiC particulate infiltrated with an Al-0.7wt%Sr alloy (circles) and of alumina particulate infiltrated with an Al-4wt%Mg alloy (squares).

Al-Mg/alumina system

The experimental results for the infiltrated height versus applied pressure for the Al-Mg alloy are shown in Fig. 1. The estimated threshold pressure is given in Table 2. Again the increase in P_0 is opposed to what the surface tension of the alloy would have indicated (see also Table 2). In this case, however, we note a very fast increase of the infiltrated height beyond P_0. This is likely due to a blocking of the entrance caused by the reaction products formed in the reaction between Mg and alumina. The latter would have surely occurred during the heating period of the sample (immersed in the melt). The results can then be rationalized by noting that the blocking of the entrance explains, on one side, the apparent increase in the threshold pressure. On the other hand, once infiltration is initiated, filling should occur at an abnormally high pace, as the pressure drop is well above threshold. Note that the system Al-Mg/SiC, in which no extensive reaction is expected to occur, behaves similarly to Al-Sn and Al-Pb alloys (Table 2). Comparison of these results with those for Al-Sr/SiC will help in identifying possible effects due to changes in the oxide layer (see below).

DISCUSSION

The capillary law and the oxide layer

The threshold pressure P_0 for infiltration is related to the surface tension of the infiltrating liquid and the contact angle at the liquid/solid interface through the so-called capillary law [4]

$$P_0 = 6\eta\gamma_{lv}\cos\theta\frac{V_p}{\left(1-V_p\right)D} \qquad (1)$$

where γ_{lv} is the liquid-vapour surface tension, θ the contact angle and η a factor which depends on the geometry of the particulate. D and V_p are the mean diameter and volume fraction of the particulate, respectively, (see Table 1). This equation indicates that the changes in the threshold pressure observed in this work could either due to changes in the surface tension of the infiltrating alloy or in the contact angle. The product $\gamma_{lv}\cos\theta$ is related to the difference between the interfacial tensions at the solid/vapor and solid/liquid interfaces through Young's equation,

$$\gamma_{lv}\cos\theta = \gamma_{sv} - \gamma_{sl} \qquad (2)$$

Thus, as γ_{sv} is hardly modified in the present case, a change in the threshold pressure would imply a change in γ_{sl}. An alternative explanation is the modification of the surface condition of liquid aluminum, and, in particular, of the characteristics of the oxide layer that covers its surface. In the following both possibilities are explored to some extent. The first possibility will be considered for Al-Sn and Al-Pb alloys, whereas the role of the second will be assessed by comparing the experimental results for Al-Sr and Al-Mg alloys.

Table 3: Experimental data for liquid/vapor surface tensions γ_{lv} [9,11] and for contact angle [12-16] and work of adhesion W on Al_2O_3 [16,17] of the liquid metals relevant to the present discussion.

Metal	T (K)	γ_{lv} (mJ.m^{-2})	θ	W (mJ m^{-2})
Al	1023	862	109º	724
	1273	832	80º	874
Sn	1023	508	145º	83
	1273	487	135º	120
Pb	1023	413	141º	71
	1273	378	132º	120

Estimation of adsorption energies

To investigate whether a given element is tensioactive at the solid/liquid interface we borrow the phenomenological theory discussed in Ref. [10]. The approach is based upon the calculation of the adsorption energy of the solid/liquid interface for a Al-X binary alloy. This energy can be written as [10],

$$E_{sl} = E_{lv} - \left(W^X - W^{Al}\right)\Omega \qquad (3)$$

where E_{lv} is the liquid/vapor adsorption energy, Ω the average surface area per mole, and W the

work of adhesion of a given liquid (l) on solid s. The liquid/vapor adsorption energy E_{lv} can in its turn be calculated by means of

$$E_{lv} = \left(\gamma_{lv}^{X} - \gamma_{lv}^{Al}\right)\Omega - m\lambda \qquad (4)$$

where λ is the regular solution parameter, and m a structural parameter which will be taken equal to 0.25 [10].

We have used this approach to investigate the Al-Sn and Al-Pb/alumina interfaces. The required experimental data for the surface tension, contact angle and work of adhesion are reported in Table 3. For the average molar surface area Ω we took its value for pure aluminium, instead of some average of their values for the two elements forming the alloy, as done in [17]. This is justified by the fact that we are only discussing dilute alloys. The regular solution parameter λ was calculated from the arithmetic mean of the tabulated partial mixing enthalpies of the binary alloys at infinite dilution [18]. The actual value of this magnitude used in the calculations, along with that of Ω are given in Table 3.

The adsorption energies obtained by this approach for two temperatures are shown in Table 4. The results indicate that neither Sn nor Pb are tensioactive at the Al/alumina interface. Thus, no change in the solid/liquid surface tension is expected. Note that the results do not significantly depend on temperature due to the fact that the interface data (Table 3) correspond to low oxidation conditions; otherwise sharp changes in contact angle and work of adhesion in the system Al/alumina have been observed when the temperature is raised from 1023 to 1273 K [17]. The significance of the results of Table 4 can be also assessed by noting that both systems are characterized by having $E_{lv} < 0 < E_{sl}$. In these systems, the alloying element is expected to increase the contact angle (in the non wetting case) and decrease the surface tension [10] so that the product $\gamma_{lv}\cos\theta$ remains almost constant. This is in agreement with experimental results obtained in high vacuum by means of the sessile drop method [12] for the Al-Sn system. This conclusion is clearly incompatible with the results for the threshold pressure shown in Table 2, as indicated by the capillary law (see Eq. (1)). Thus, we may conclude that the experimental results for the changes induced in the threshold pressure by tin and lead additions can be hardly interpreted in terms of experimental data obtained under low oxidation conditions (high vacuum) or phenomenological theories which do not explicitly account for effects related to the oxide layer.

Table 4: Calculated adsorption energies E_{lv} and E_{sl} (see text) for Al-Sn and Al-Pb alloys on Al_2O_3 and experimental data for two of the parameters used in the calculation (see Eqs. (3) and (4)).

Alloy	T (K)	λ (kJ mol^{-1})	Ω (10^4 m^2 mol^{-1})	E_{lv} (kJ mol^{-1})	E_{sl} (kJ mol^{-1})
Al-Sn	1023	20	5.0	-22.7	9.4
	1273			-22.3	15.4
Al-Pb	1023	34	5.0	-31.0	1.7
	1273			-31.2	6.5

Effect of the oxide layer

The other possibility resides upon a strong influence of the oxide layer that covers the aluminum surface on the infiltration process. The fact that Sr additions increase P_0, notwithstanding the sharp decrease in surface tension (Table 2), can only be understood in terms of an increase in thickness or strength of the oxide film. Note that a blocking of the entrance of the compact can be readily discarded by comparing the results for Al-Sr with those for Al-Mg/alumina (see above). The analysis of the results for Sn and Pb alloys also leads to conclude that the oxide layer should play a crucial role in determining the threshold pressure, although in this case the oxide layer seems to be scarcely affected by the two additions.

CONCLUSIONS

As most infiltration experiments are carried out in an oxygen rich atmosphere, it is very likely that aluminum is covered by a rather thin oxide layer. The question is how this film affects to the infiltration process and in particular to the threshold pressure. Some authors argue that as soon as pressure is applied the oxide layer should be disrupted by the ceramic particles and that no restoration of the layer is expected during the infiltration process. Our experimental results and the analysis of previous experimental data for Al-Sn and Al-Pb alloys by means of a phenomenological theory force us to the opposite conclusion, namely that the oxide layer plays an essential role in the infiltration process and in particular in determining the threshold pressure for infiltration. The film should play a role not only at threshold but also along the whole infiltration process, as, otherwise, a sharp increase in infiltration height versus pressure should have been observed (as in the Al-Mg/alumina system). These conclusions are in line with results of the present authors on the effects of coating SiC particulate with K_2ZrF_6, temperature or infiltration atmosphere, on pressure infiltration.

ACKNOWLEDGMENTS

This work was supported in part by the Spanish CICYT (grant MAT96-1048). C. García-Cordovilla is thankful to the "Industria Española del Aluminio" for permission to publish this work.

REFERENCES

1. Mortensen, A., and Jin, I., “Solidification processing of metal matrix comoposites”, *Int. Mater. Rev.*, vol. 37, 1992, pp. 101-128.
2. Alonso, A., Narciso, J., Pamies, A., García-Cordovilla, C., and Louis, E., “Effect of K_2ZrF_6 coatings on pressure infiltration of packed SiC particulate by liquid aluminum”, *Scripta Metall. Et Mater.*, vol. 29, 1993, pp. 1559-1564.
3. Narciso, J., García-Cordovilla, C., and Louis, E., “Effects of Temperature on pressure infiltration of packed SiC particulates by liquid aluminum”, *J. Mater. Sci. Lett.*, Vol. 14,

1995, pp. 1144-1146.
4. Narciso, J., Alonso, A., Pamies, A., García-Cordovilla, C., and Louis, E., " Factors affecting pressure infiltration of packed SiC particulate by liquid aluminum", *Metall et Mater. Trans. A*, vol. 26A, 1995, pp. 983-990.
5. Alonso, A., Pamies, A., Narciso, J., García-Cordovilla, C., and Louis, E., "Evaluation of the wettability of liquid aluminium with ceramic particulates (SiC, TiC, Al_2O_3) by means of pressure infiltration", *Metall. Trans. A*, vol. 24A, 1993, pp. 1423-1432.
6. Alonso, A., Garcia-Cordovilla, C., Louis, E., Narciso, J., and Pamies, A., "Evaluation of the wettability of Al-Pb and Al-Sn alloys with SiC and Al2O3 particulate by means of pressure infiltration", *J. Mater. Sci.*, Vol. 29, 1994, pp. 4729-4735.
7. Lang, G., *Aluminium*, vol. 49, 1973, pp. 231-238; *ibid*, vol. 50, 1974, pp. 731-734.
8. Goumiri, J., Joud, J.C., Desre, P., and Hicter, J.M., "Tensions superficielles d'alliages liquides binaires preséntant un charactère d'immiscibilité: Al-Pb, Al-Bi, Al-Sn et Zn-Bi", *Surf. Sci.*, vol. 83, 1979, pp. 471-486.
9. Pamies, A., García-Cordovilla, C., and Louis, E., "The measurement of the surface tension of liquid aluminium by means of the maximum bubble pressure method": the effect of surface oxidation", *Scripta Metall.* vol. 18, 1984, pp. 869-872.
10. Li, J.G., Coudurier, L., and Eustathopoulos, N., "Work of adhesion and contact-angle isotherm of binary alloys on ionocovalent oxides", *J. Mater. Sci.*, Vol. 24, 1989, pp. 1109-1116.
11. Lucas, L.D., *Techniques de l'ingénieur*, Paris, 1984, M67 et M65.
12. Li, J.G., Chatain, D., Coudurier, L., and Eustathopoulos, N., *J. Mater. Sci. Lett.*, vol. 7, 1988, p. 961.
13. Chatain, D., Rivollet, I., and Eustathopoulos, N., "Adhesion Thermodynamique dans les systemes non-reactifs metal-liquide-alumine", *J. Chim. Phys.*, Vol. 83, 1986, pp. 561-567.
14. Coudurier, L., Adorian, J., Pique, D., and Eustathopoulos, N., "Etude de la mouillabilité par l'aluminium liquide de l'alumine recouverte d'une couche de métal ou de composé réfractaire", *Rev. Int. Hautes Tempér Réfract.*, vol. 21, 1984, pp. 81-93.
15. Laurent, V., Chatain, D., Chatillon, C., and Eustathopoulos, N., "Wettability of monocrystalline alumina by aluminium between its melting point and 1273 K", *Acta Metall.*, Vol. 36, 1988, pp. 1797-1803.
16. Nikolopoulos, P., Sotiropoulou, and Ondracek, G., "Temperature dependence of interfacial energies between solid oxide ceramics and liquid metals", *J. Therm. Anal.*, Vol. 33, 1988, pp. 633-642.
17. Chatain, D., Coudurier, L., and Eustathopoulos, N., "Wetting and interfacial bonding in ionocovalent oxide-liquid metal systems", *Revue Phys. Appl.*, Vol. 23, 1988, pp. 1055-1064.
18. Hultgren, R., Desai, P.D., Hawkins, D.T., Gleiser, M., and Kelly, K.K., *Selected values of the Thermodynamic Properties of Binary Alloys*, American Society for Metals, Ohio, 1973.